Journal of Computational and Applied Mathematics 234 (2010) 73–94

Contents lists available at ScienceDirect

Journal of Computational and Applied Mathematics

journal homepage: www.elsevier.com/locate/cam

An interpolation matched interface and boundary method for elliptic interface problems☆

Kejia Pan[a,b,*], Yongji Tan[b], Hongling Hu[c]

[a] School of Mathematical Sciences and Computing Technology, Central South University, Changsha, Hunan, 410075, China
[b] School of Mathematical Sciences, Fudan University, Shanghai 200433, China
[c] College of Mathematics and Computer Science, Hunan Normal University, Changsha, Hunan, 410081, China

ARTICLE INFO

Article history:
Received 23 September 2008
Received in revised form 13 October 2009

MSC:
65N06
65N22
65N50

Keywords:
Ghost fluid method
Immersed interface method
Matched interface and boundary
Elliptic interface problems
Finite difference scheme
Discrete maximum principle

ABSTRACT

An interpolation matched interface and boundary (IMIB) method with second-order accuracy is developed for elliptic interface problems on Cartesian grids, based on original MIB method proposed by Zhou et al. [Y. Zhou, G. Wei, On the fictious-domain and interpolation formulations of the matched interface and boundary method, J. Comput. Phys. 219 (2006) 228–246]. Explicit and symmetric finite difference formulas at irregular grid points are derived by virtue of the level set function. The difference scheme using IMIB method is shown to satisfy the discrete maximum principle for a certain class of problems. Rigorous error analyses are given for the IMIB method applied to one-dimensional (1D) problems with piecewise constant coefficients and two-dimensional (2D) problems with singular sources. Comparison functions are constructed to obtain a sharp error bound for 1D approximate solutions. Furthermore, we compare the ghost fluid method (GFM), immersed interface method (IIM), MIB and IMIB methods for 1D problems. Finally, numerical examples are provided to show the efficiency and robustness of the proposed method.
© 2009 Elsevier B.V. All rights reserved.

1. Introduction

Consider the elliptic equation

$$\nabla \cdot \big(\beta(\mathbf{x})\nabla u(\mathbf{x})\big) = f(\mathbf{x}) \quad \mathbf{x} \in \Omega = \Omega^+ \cup \Omega^- \tag{1.1}$$

with a Dirichlet, Neumann or mixed boundary condition prescribed on $\partial\Omega$. For simplicity, Ω is assumed to be a regular domain, such as rectangle in two-dimensions (2D) or cuboid in three-dimensions (3D). Across some smooth interface Γ in domain Ω, the coefficient function $\beta(\mathbf{x})$ of the elliptic equation is discontinuous, while the source term $f(\mathbf{x})$ may be even singular. Depending on the properties of $f(\mathbf{x})$, we usually have jump conditions across the interface Γ:

$$[u]_\Gamma = u^+(\mathbf{x}) - u^-(\mathbf{x}) = a(\mathbf{x}), \qquad [\beta u_n]_\Gamma = \beta^+(\mathbf{x})u_n^+(\mathbf{x}) - \beta^-(\mathbf{x})u_n^-(\mathbf{x}) = b(\mathbf{x}) \tag{1.2}$$

where $\mathbf{x}$ is a point on the interface Γ, n is the unit outer normal direction. The superscript $-$ or $+$, denotes the limiting value of a function from one side or the other of the interface.

☆ This work was supported by Chinese NSF Project 10431030.
* Corresponding author at: School of Mathematical Sciences and Computing Technology, Central South University, Changsha, Hunan, 410075, China.
E-mail addresses: kjpan@yahoo.cn (K. Pan), yjtan@fudan.edu.cn (Y. Tan), honglinghu@yahoo.cn (H. Hu).

0377-0427/$ – see front matter © 2009 Elsevier B.V. All rights reserved.
doi:10.1016/j.cam.2009.12.006

Such elliptic interface problems often arise in fluid dynamics, molecular biology, electromagnetics and material science, and many efficient numerical methods for these problems have been developed. The discussion of existence and regularity of the solution to the interface problem can be found in [1,2]. There is also a vast amount of literature on numerical schemes and error analysis for the problem (1.1) and (1.2), such as Peskin's immersed boundary method (IBM) [3–8], the IIM [9–19], the GFM [20–22], the MIB method [23–27], finite element method (FEM) [1,28,2,29–32] and some other body-fitting approaches [33,34]. For certain geometrically complex domain, the consumption of a good body-fitting mesh remains a nontrivial and time-consuming task, even though considerable progress has been made. Furthermore, a considerable increase of the computational difficulty will be encountered for free interface problems, where a moving mesh method is required to regenerate the grid during the simulation. However, sharp interface methods such as the IIM, GFM and MIB method use fixed Cartesian grids, thus they can easily be used to simulate dynamical problems in conjunction with the level set function, which describes the motion of the interface in an elegant and simple way. Therefore, sharp interface methods are more suitable and promising than body-fitting approaches for such interface problems.

For this class of problems, apart from the pioneer work of Peskin [5] in 1977, a number of other elegant methods have been proposed. Among them, the IIM proposed by Leveque and Li [12] is one of the most popular and powerful methods which are designed to preserve interface jumps in solving elliptic equations. The IIM is the first sharp interface method and is the first second-order method, although its local truncation error at irregular points is of $O(h)$. The IIM uses local Taylor expansions around a set of control points on the interface and determines the weights of the neighboring points by matching the interface conditions to high order. However, for 2D or 3D problems, a local coordinate is typically required to offer a better representation of the jump conditions since they are usually given in the direction normal to the interface. In the original IIM, the coefficients and the correction terms in the finite difference formulas at irregular points cannot be obtained explicitly, instead, they are often computed numerically by solving a linear equations system. In addition, the schemes in the vicinity of the interface have to vary from point to point. This complicated procedure becomes a barrier to solving complex 2D or 3D dynamical problems.

The GFM was originally designed to treat contact discontinuities in the inviscid Euler equations [20]. In favor of the level set method, the interface jump conditions are captured implicitly by extending values across the interface into a ghost fluid. In high dimensions, the jump in the normal derivative is correctly captured through a projection to Cartesian coordinate directions, while the less important jump in the tangential directions is neglected. Such a modeling is in consistent with its overall first-order accuracy. In the GFM, the interface jump conditions are applied on the nearest grid points of an interface, instead of at the exact interface position. This treatment generates a symmetric matrix for the associated linear system, and thus standard techniques of acceleration such as preconditioned conjugate gradient (PCG) and multigrid can be used to invert the matrix. From this point of view, the GFM is very simple and easy to use for complex interface problems.

Another popular sharp interface method MIB proposed by Zhou et al. [26], which can be regarded as a higher-order generalization of the IIM and the GFM, is quite robust and efficient, of arbitrarily high-order accuracy in principle. The earliest version of the MIB method was proposed in [25] by Zhao and Wei. The MIB method has been developed in Wei's group over past few years. Most recently, Yu, Zhou and Wei generalize their original MIB method to treat geometric singularities [23,24]. And the application of such MIB method to the electrostatic analysis of biomolecules is reported elsewhere [35]. The MIB approach makes use of fictitious domains so that standard central finite difference scheme can be applied across the interface without loss of accuracy. The values on the fictitious domains are determined simultaneously from enforcing the interface jump conditions at the exact position of the interface. One feature of the MIB is that it disassociates between the discretization of the equation and the enforcement of interface jump conditions. Another feature is to just make repeated use of the lowest-order interface jump conditions to achieve high-order accuracy.

The convergence and error estimations are also very important for sharp interface schemes. A convergence proof for the GFM is provided in [36]. The error analysis is given for the IIM applied to 1D elliptic interface problems using both the comparison functions and asymptotic analysis; however, no rigorous proof is given for 2D case [19]. A maximum principle preserving immersed interface method (MIIM) [13] is second-order accurate with complete theoretical proof. However, the use of an optimization scheme to force the maximum principle is somewhat complicated. And till now there is no theoretical proof of convergence of the MIB method for elliptic interface problems.

The object of this paper is to propose a simple finite difference scheme named IMIB for solving elliptic interface problems on Cartesian grids. The IMIB method is similar to the interpolation formulation in [27], which use the Lagrange polynomial to compute the required coefficients at any given order. The IMIB method reformulate the MIB method, and result in symmetric and explicit difference formulas at second-order accuracy, while the original MIB formulas are not explicitly derived, instead, they are computed by a computer program. For elliptic interface problems with constant coefficients, the resulting matrices are just the same as the case without interfaces; for 1D interface problems with piecewise constant coefficients, the resulting matrices are symmetric and positive definite. It is easy to obtain the second-order convergence of the IMIB method applied to 1D problems with piecewise constant coefficients and 2D problems with constant coefficients by comparison functions technique. Because of its simplicity, it can be easily generalized to solve high-dimensional and dynamical problems. Furthermore, it is easily seen the relation among the GFM, IIM, MIB and IMIB method in 1D from the derivation of our method. However, in higher dimensions, these methods differ very much in many aspects; see [27] for details.

The rest of this paper is organized as follows. In Section 2, we first explain our ideas and derive the corresponding formulas for 1D problems, then briefly explain how to solve high dimension problems. Convergence analysis for the IMIB method is presented in Section 3. Finally, we show the numerical results of some test problems in Section 4, and formulas in Section 5.

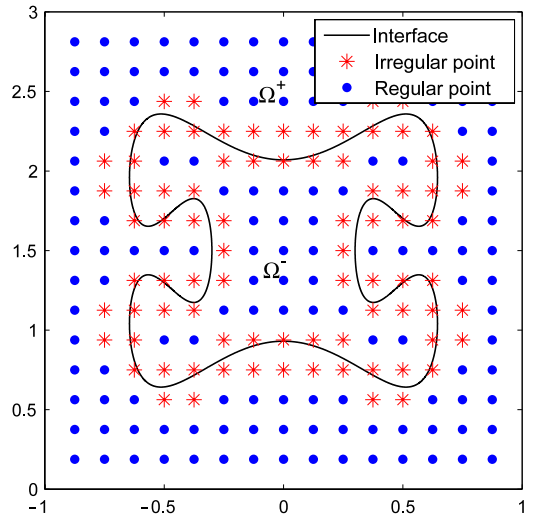

Fig. 1. Computational domains and interfaces with uniform Cartesian grids.

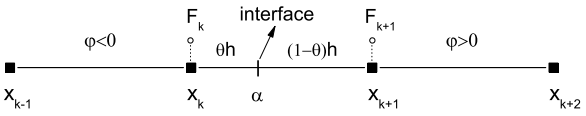

Fig. 2. The local configuration near interface.

2. Numerical method

Since the interface can have a fairly complex shape, the interface location is represented by the zero level set of a signed distance function ϕ. Meanwhile, the set of all points where $\phi < 0$ and the set of all points where $\phi > 0$ represent two disjoint subdomains, Ω^- and Ω^+, respectively. For the numerical algorithm, we identify whether the point is located in Ω^- or Ω^+ by considering the local sign of ϕ, unless $\phi = 0$ implying that the point is located exactly on the interface.

As shown in Fig. 1, we take a uniform grid on the regular domain Ω. We define the *irregular point* as the one at which all the discretization points in a standard central finite difference scheme are not on the same side of the interface. For example, in a second-order 2D scheme, an irregular point has at least one of its nearest neighbor grid points lying on the other side of the interface.

2.1. The 1D Poisson equation

Consider the 1D Poisson equation

$$u_{xx} = f(x) \tag{2.1}$$

with Dirichlet boundary conditions on $\partial\Omega$. We notice that only irregular points necessitate special care when standard central difference scheme is applied to the whole domain. For each regular grid point i, the standard second-order discretization

$$\frac{u_{i+1} - 2u_i + u_{i-1}}{h^2} = f_i \tag{2.2}$$

can be used. For irregular grid points, we should modify standard difference discretization to maintain the jump conditions.

In favor of the level set function ϕ, we can identify the location of the interface as follow. Assume that the interface lies between x_k and x_{k+1}, and $[u]_\Gamma = a_\Gamma$ and $[u_x]_\Gamma = b_\Gamma$, then

$$\theta = \frac{|\phi_k|}{|\phi_k| + |\phi_{k+1}|} \tag{2.3}$$

can be used to estimate the interface location. That is, the interface splits this cell into two pieces with size θh on the left and size $(1-\theta)h$ on the right. Because the derivative approximation at the irregular grid points x_k and x_{k+1} refer to points from the other side of the interface, two fictitious values F_k and F_{k+1} in place of real ones should be supplied, as shown in Fig. 2.

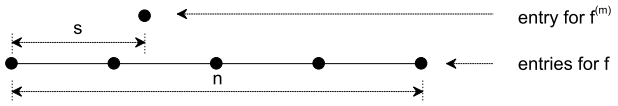

Fig. 3. Schematic illustration of how the notation used in the Taylor weight algorithm relates to stencil shape; here shown in a staggered case with $s = 1.3$, $n = 3$.

Table 1
Input parameters to the Mathematics for the four cases.

Case	m	s	n
u_Γ^-	0	$1+\theta$	2
u_Γ^+	0	θ	2
$u_\Gamma'^-$	1	$1+\theta$	2
$u_\Gamma'^+$	1	θ	2

By the use of Taylor weight algorithm (see [37]), the approximations of the values of u and its derivatives on the left and the right side of the interface can be written as

$$u_\Gamma^- = \left(-\frac{\theta}{2}+\frac{\theta^2}{2}\right)u_{k-1} + (1-\theta^2)u_k + \left(\frac{\theta}{2}+\frac{\theta^2}{2}\right)F_{k+1} \tag{2.4}$$

$$u_\Gamma^+ = \left(1-\frac{3}{2}\theta+\frac{\theta^2}{2}\right)F_k + (2\theta-\theta^2)u_{k+1} + \left(-\frac{\theta}{2}+\frac{\theta^2}{2}\right)u_{k+2} \tag{2.5}$$

and

$$u_\Gamma'^- = \left[\left(-\frac{1}{2}+\theta\right)u_{k-1} - 2\theta u_k + \left(\frac{1}{2}+\theta\right)F_{k+1}\right] \Big/ h \tag{2.6}$$

$$u_\Gamma'^+ = \left[\left(-\frac{3}{2}+\theta\right)F_k + (2-2\theta)u_{k+1} - \left(\frac{1}{2}-\theta\right)u_{k+2}\right] \Big/ h \tag{2.7}$$

respectively. These weights are obtained by executing the Mathematica statement

```
CoefficientList[Normal[Series[x^s*Log[x]^m,{x,1,n}]/h^m],x]
```

where

m order of derivative to be approximated,
s number of grid intervals in between the derivative and function entries; select the sign "+" if the former is to the right of the latter, else the sign "−",
n number of grid intervals in between left- and rightmost function entries;

cf. Fig. 3. We choose the parameters as shown in Table 1, then obtain (2.4)–(2.7).

In order to determine two fictitious values F_k and F_{k+1}, we discretize two jump conditions as

$$\begin{aligned}&\left(-\frac{\theta}{2}+\frac{\theta^2}{2}\right)u_{k-1} + (1-\theta^2)u_k + \left(\frac{\theta}{2}+\frac{\theta^2}{2}\right)F_{k+1}\\ &\quad= \left(1-\frac{3}{2}\theta+\frac{\theta^2}{2}\right)F_k + (2\theta-\theta^2)u_{k+1} + \left(-\frac{\theta}{2}+\frac{\theta^2}{2}\right)u_{k+2} - a_\Gamma,\end{aligned} \tag{2.8}$$

$$\left(-\frac{1}{2}+\theta\right)u_{k-1} - 2\theta u_k + \left(\frac{1}{2}+\theta\right)F_{k+1} = \left(-\frac{3}{2}+\theta\right)F_k + (2-2\theta)u_{k+1} - \left(\frac{1}{2}-\theta\right)u_{k+2} - b_\Gamma h, \tag{2.9}$$

which can be rewritten as

$$\begin{aligned}&\left(1-\frac{3}{2}\theta+\frac{\theta^2}{2}\right)F_k - \left(\frac{\theta}{2}+\frac{\theta^2}{2}\right)F_{k+1}\\ &\quad= \left(-\frac{\theta}{2}+\frac{\theta^2}{2}\right)u_{k-1} + (1-\theta^2)u_k - (2\theta-\theta^2)u_{k+1} + \left(\frac{\theta}{2}-\frac{\theta^2}{2}\right)u_{k+2} + a_\Gamma,\end{aligned} \tag{2.10}$$

$$\left(-\frac{3}{2}+\theta\right)F_k - \left(\frac{1}{2}+\theta\right)F_{k+1} = \left(-\frac{1}{2}+\theta\right)u_{k-1} - 2\theta u_k - (2-2\theta)u_{k+1} + \left(\frac{1}{2}-\theta\right)u_{k+2} + b_\Gamma h. \tag{2.11}$$

From (2.10) and (2.11), we can easily get the explicit expressions for two unknowns F_k and F_{k+1}:

$$F_k = \frac{-\theta^2 u_{k-1} + (1+\theta)^2 u_k - 3\theta^2 u_{k+1} + \theta^2 u_{k+2} + (1+2\theta)a_\Gamma - (\theta+\theta^2)b_\Gamma h}{1+2\theta-2\theta^2}, \tag{2.12}$$

$$F_{k+1} = \frac{(1-\theta)^2 u_{k-1} - 3(1-\theta)^2 u_k + (2-\theta)^2 u_{k+1} - (1-\theta)^2 u_{k+2} - (3-2\theta)a_\Gamma - (2-3\theta+\theta^2)b_\Gamma h}{1+2\theta-2\theta^2}, \tag{2.13}$$

where $1+2\theta-2\theta^2 = -2(\theta-\frac{1}{2})^2 + \frac{3}{2} > 1$. With these two expansions of F_k and F_{k+1}, we could discretize u_{xx} at irregular grid points x_k and x_{k+1} as at regular point

$$\left[\left(\frac{F_{k+1}-u_k}{h}\right) - \left(\frac{u_k - u_{k-1}}{h}\right)\right] \Big/ h = f_k, \tag{2.14}$$

$$\left[\left(\frac{u_{k+2}-u_{k+1}}{h}\right) - \left(\frac{u_{k+1} - F_k}{h}\right)\right] \Big/ h = f_{k+1}. \tag{2.15}$$

Through a perfectly simple calculation, we obtain the modified finite difference scheme

$$\begin{aligned}&(2-\theta^2)u_{k-1} - (5-2\theta-\theta^2)u_k + (2-\theta)^2 u_{k+1} - (1-\theta)^2 u_{k+2}\\ &\quad = (3-2\theta)a_\Gamma + (2-3\theta+\theta^2)b_\Gamma h + (1+2\theta-2\theta^2)h^2 f_k\end{aligned} \tag{2.16}$$

and

$$\begin{aligned}&-\theta^2 u_{k-1} + (1+\theta)^2 u_k - (2+4\theta-\theta^2)u_{k+1} + (1+2\theta-\theta^2)u_{k+2}\\ &\quad = -(1+2\theta)a_\Gamma + (\theta+\theta^2)b_\Gamma h + (1+2\theta-2\theta^2)h^2 f_{k+1}\end{aligned} \tag{2.17}$$

at irregular grid points x_k and x_{k+1}, respectively. We can rewrite (2.16) and (2.17) as

$$\frac{u_{k+1}-2u_k+u_{k-1}}{h^2} = \tilde{f}_k + \frac{a_\Gamma}{h^2} + \frac{b_\Gamma(1-\theta)}{h} \tag{2.18}$$

and

$$\frac{u_{k+2}-2u_{k+1}+u_k}{h^2} = \tilde{f}_{k+1} - \frac{a_\Gamma}{h^2} + \frac{b_\Gamma\theta}{h} \tag{2.19}$$

where

$$\tilde{f}_k = \frac{1+2\theta-\theta^2}{2} f_k + \frac{(1-\theta)^2}{2} f_{k+1}, \tag{2.20}$$

$$\tilde{f}_{k+1} = \frac{\theta^2}{2} f_k + \frac{2-\theta^2}{2} f_{k+1}. \tag{2.21}$$

Considering $f_{k+1} = f_k + [f]_\Gamma + O(h)$, the difference schemes above can be simplified as follows:

$$\frac{u_{k+1}-2u_k+u_{k-1}}{h^2} = f_k + \frac{a_\Gamma}{h^2} + \frac{b_\Gamma(1-\theta)}{h} + \frac{[f]_\Gamma(1-\theta)^2}{2}, \tag{2.22}$$

and

$$\frac{u_{k+2}-2u_{k+1}+u_k}{h^2} = f_{k+1} - \frac{a_\Gamma}{h^2} + \frac{b_\Gamma\theta}{h} - \frac{[f]_\Gamma\theta^2}{2}, \tag{2.23}$$

from which we can find that the standard central difference scheme can be applied in the whole domain, the only difference is that we need to modify the right-hand side of the resulting linear system to model the singular source.

Remark 2.1. Difference schemes (2.16) and (2.17) are just the same as original second-order MIB [26] method. Difference formulations (2.22) and (2.23) are essentially equivalent to the IIM [12] and interpolation formulation [27]. Furthermore, if $[f]_\Gamma = 0$, difference formulations (2.22) and (2.23) are just the same as the GFM [21].

2.2. The 1D Quasi-Poisson equation

Consider the 1D variable coefficient Poisson equation

$$(\beta u_x)_x = f(x) \tag{2.24}$$

with interface jump conditions, $[u]_\Gamma = a_\Gamma$ and $[\beta u_x]_\Gamma = b_\Gamma$. The standard second-order discretization for each regular grid point i becomes

$$\left[\beta_{i+1/2}\left(\frac{u_{i+1}-u_i}{h}\right)-\beta_{i-1/2}\left(\frac{u_i-u_{i-1}}{h}\right)\right]\Big/h = f_i \tag{2.25}$$

where $\beta_{i\pm1/2} = \beta(x_{i\pm1/2})$. To simplify the presentation we assume that the coefficient β is a piecewise constant, i.e., $\beta = \beta^-$ if $x \in \Omega^-$ and $\beta = \beta^+$ if $x \in \Omega^+$, while our new method for general piecewise continuous β is almost identical. In practical problems β often represents a physical quantity such as conductivity, permeability, or density and so $\beta > 0$, $r = \beta^+/\beta^- > 0$ everywhere. By discretizing the jump conditions in the same way, two fictitious values F_k and F_{k+1}, as shown in Fig. 2, can be determined via

$$\begin{aligned}&\left(-\frac{\theta}{2}+\frac{\theta^2}{2}\right)u_{k-1}+(1-\theta^2)u_k+\left(\frac{\theta}{2}+\frac{\theta^2}{2}\right)F_{k+1}\\&=\left(1-\frac{3}{2}\theta+\frac{\theta^2}{2}\right)F_k+(2\theta-\theta^2)u_{k+1}+\left(-\frac{\theta}{2}+\frac{\theta^2}{2}\right)u_{k+2}-a_\Gamma\end{aligned} \tag{2.26}$$

$$\begin{aligned}&\beta^-\left(\left(-\frac{1}{2}+\theta\right)u_{k-1}-2\theta u_k+\left(\frac{1}{2}+\theta\right)F_{k+1}\right)\\&=\beta^+\left(\left(-\frac{3}{2}+\theta\right)F_k+(2-2\theta)u_{k+1}-\left(\frac{1}{2}-\theta\right)u_{k+2}\right)-b_\Gamma h\end{aligned} \tag{2.27}$$

in place of (2.8) and (2.9).

Solving (2.26) and (2.27) gives

$$\begin{aligned}F_k \;=\; &\big(-2\theta^2u_{k-1}+2(\theta+1)^2u_k+2\theta(2\theta^2-3\theta-2-2r\theta^2+2r)u_{k+1}-\theta(2\theta^2-\theta-1-2r\theta^2-r\theta+r)u_{k+2}\\&+2(2\theta+1)a_\Gamma-2\theta(\theta+1)b_\Gamma h\big)/\big((2+\theta-5\theta^2+2\theta^3)+r(3+\theta-2\theta^2)\theta\big),\end{aligned} \tag{2.28}$$

$$\begin{aligned}F_{k+1} \;=\; &\big(-(\theta-1)(2\theta^2-5\theta+2-2r\theta^2+3r\theta)u_{k-1}+2(\theta-1)(2\theta^2-4\theta+3r-2r\theta^2+r\theta)u_k\\&+2r(\theta-2)^2u_{k+1}-2r(\theta-1)^2u_{k+2}+2r(2\theta-3)a_\Gamma-2(\theta-1)(\theta-2)b_\Gamma h\big)\\&/\big((2+\theta-5\theta^2+2\theta^3)+r(3+\theta-2\theta^2)\theta\big),\end{aligned} \tag{2.29}$$

where $(2+\theta-5\theta^2+2\theta^3)+r(3+\theta-2\theta^2)\theta = (1-\theta)(2-\theta)(1+2\theta)+r(1+\theta)(3-2\theta) > 2r$. Then, substituting (2.28) and (2.29) into

$$\left[\beta_{k+1/2}\left(\frac{F_{k+1}-u_k}{h}\right)-\beta_{k-1/2}\left(\frac{u_k-u_{k-1}}{h}\right)\right]\Big/h = f_k \tag{2.30}$$

$$\left[\beta_{k+3/2}\left(\frac{u_{k+2}-u_{k+1}}{h}\right)-\beta_{k+1/2}\left(\frac{u_{k+1}-F_k}{h}\right)\right]\Big/h = f_{k+1} \tag{2.31}$$

leads to

$$\begin{aligned}&(2/r+3\theta-3\theta/r-2\theta^2+\theta^2/r)u_{k-1}-(3+2/r+\theta-3\theta/r-2\theta^2+\theta^2/r)u_k+(2-\theta)^2u_{k+1}-(1-\theta)^2u_{k+2}\\&=(3-2\theta)a_\Gamma+(2-3\theta+\theta^2)b_\Gamma h/\beta^+ +(2/r+\theta/r+3\theta-5\theta^2/r+\theta^2+2\theta^3/r-2\theta^3)(h)^2f_k/(2\beta^-)\end{aligned} \tag{2.32}$$

and

$$\begin{aligned}&-\theta^2u_{k-1}+(1+\theta)^2u_k-(2+3\theta+r\theta+r\theta^2-2\theta^2)u_{k+1}+(1+\theta+r\theta+r\theta^2-2\theta^2)u_{k+2}\\&=-(1+2\theta)a_\Gamma+(\theta+\theta^2)b_\Gamma h/\beta^- +(2+\theta+3r\theta-5\theta^2+r\theta^2+2\theta^3-2r\theta^3)h^2f_{k+1}/(2\beta^+)\end{aligned} \tag{2.33}$$

as the equations for the unknowns u_k and u_{k+1}, respectively. Setting

$$\hat\beta = \frac{\beta^+\beta^-}{\beta^+\theta+\beta^-(1-\theta)}, \tag{2.34}$$

we can rewrite (2.32) and (2.33) as

$$\left[\hat\beta\left(\frac{u_{k+1}-u_k}{h}\right)-\beta^-\left(\frac{u_k-u_{k-1}}{h}\right)\right]\Big/h = \tilde f_k+\frac{\hat\beta a_\Gamma}{h^2}+\frac{\hat\beta(1-\theta)b_\Gamma}{\beta^+h} \tag{2.35}$$

and

$$\left[\beta^+\left(\frac{u_{k+2}-u_{k+1}}{h}\right)-\hat\beta\left(\frac{u_{k+1}-u_k}{h}\right)\right]\Big/h = \tilde f_{k+1}-\frac{\hat\beta a_\Gamma}{h^2}+\frac{\hat\beta\theta b_\Gamma}{\beta^-h} \tag{2.36}$$

to emphasize that this numerical method yields a symmetric linear system with $\beta_{k+1/2} = \hat{\beta}$. Here,

$$\tilde{f}_k = \frac{\hat{\beta}}{2}\left(\frac{\theta+\theta^2}{\beta^-} + \frac{1+\theta-2\theta^2}{\beta^+}\right) f_k + \frac{\hat{\beta}(1-\theta)^2}{2\beta^+} f_{k+1}, \tag{2.37}$$

$$\tilde{f}_{k+1} = \frac{\hat{\beta}\theta^2}{2\beta^-} f_k + \frac{\hat{\beta}}{2}\left(\frac{2-3\theta+\theta^2}{\beta^+} + \frac{3\theta-2\theta^2}{\beta^-}\right) f_{k+1}. \tag{2.38}$$

From the fact that $f_{k+1} = f_k + [f]_\Gamma + O(h)$, the expressions above can be rewritten as

$$\tilde{f}_k = \frac{\hat{\beta}}{2}\left(\frac{\theta+\theta^2}{\beta^-} + \frac{2-\theta-\theta^2}{\beta^+}\right) f_k + \frac{\hat{\beta}(1-\theta)^2}{2\beta^+}[f]_\Gamma + O(h), \tag{2.39}$$

$$\tilde{f}_{k+1} = \frac{\hat{\beta}}{2}\left(\frac{2-3\theta+\theta^2}{\beta^+} + \frac{3\theta-\theta^2}{\beta^-}\right) f_{k+1} - \frac{\hat{\beta}\theta^2}{2\beta^-}[f]_\Gamma + O(h). \tag{2.40}$$

Remark 2.2. Difference schemes (2.32) and (2.33) are the same as that in original second-order MIB [26] method. Substituting (2.39) and (2.40) into (2.35) and (2.36), we obtain the difference schemes essentially equivalent to the IIM [12] and interpolation formulation [27]; see Appendix for details. Simply setting $\tilde{f}_k = f_k, \tilde{f}_{k+1} = f_{k+1}$ gives the same schemes as the GFM [21].

2.3. The 2D Poisson equation

Consider 2D Poisson equation

$$u_{xx} + u_{yy} = f(x, y) \tag{2.41}$$

with interface jump conditions $[u]_\Gamma = a(x, y)$ and $[u_n]_\Gamma = b(x, y)$. The unit normal of the interface $\vec{n} = (n_1, n_2)$, can be defined as $\frac{\nabla\phi}{|\nabla\phi|}$ where the normal is computed at each grid node using central difference.

Before proceeding to the construction of the numerical scheme for u_{xx} or u_{yy} at irregular grid points, we first rewrite the interface jump conditions as two separate conditions for $[u_x]_\Gamma$ and $[u_y]_\Gamma$, then apply our method to 2D problems dimension by dimension.

Differentiating interface jump condition $[u]_\Gamma = a$ along the tangential direction of the interface, we obtain one more condition

$$[u_\tau]_\Gamma = a_\tau \tag{2.42}$$

where u_τ is the derivative in the tangential direction $\vec{\tau} = (-n_2, n_1)$. Hence, the derivation jump conditions can be reformulated as

$$[u_\tau]_\Gamma = (u_y^+ n_1 - u_x^+ n_2) - (u_y^- n_1 - u_x^- n_2) = [u_y]_\Gamma n_1 - [u_x]_\Gamma n_2 = a_\tau, \tag{2.43}$$

$$[u_n]_\Gamma = (u_x^+ n_1 + u_y^+ n_2) - (u_x^- n_1 + u_y^- n_2) = [u_x]_\Gamma n_1 + [u_y]_\Gamma n_2 = b. \tag{2.44}$$

Then

$$[u_x]_\Gamma = bn_1 - a_\tau n_2 \triangleq bx \tag{2.45}$$

$$[u_y]_\Gamma = a_\tau n_1 + bn_2 \triangleq by \tag{2.46}$$

follow directly from (2.43) and (2.44).

In this case, we can directly apply the general 1D formulas at irregular pints to $[u_x]_\Gamma$ and $[u_y]_\Gamma$. Discretization from (2.22) and (2.23) is called Scheme 1, discretization from (2.16) and (2.17) is called Scheme 2. To explain it more clearly, we consider three typical irregular points shown in Fig. 4.

Case a. Irregular point in ij-direction.

Define

$$\theta_x = \frac{|\phi_{i+1,j}|}{|\phi_{i,j}| + |\phi_{i+1,j}|}, \qquad \theta_y = \frac{|\phi_{i,j+1}|}{|\phi_{i,j}| + |\phi_{i,j+1}|}, \tag{2.47}$$

then

$$ax_\Gamma = \theta_x a_{i,j} + (1-\theta_x) a_{i+1,j}, \tag{2.48}$$

$$ay_\Gamma = \theta_y a_{i,j} + (1-\theta_y) a_{i,j+1}, \tag{2.49}$$

$$bx_\Gamma = \theta_x bx_{i,j} + (1-\theta_x) bx_{i+1,j}, \tag{2.50}$$

$$by_\Gamma = \theta_y by_{i,j} + (1-\theta_y) by_{i,j+1}. \tag{2.51}$$

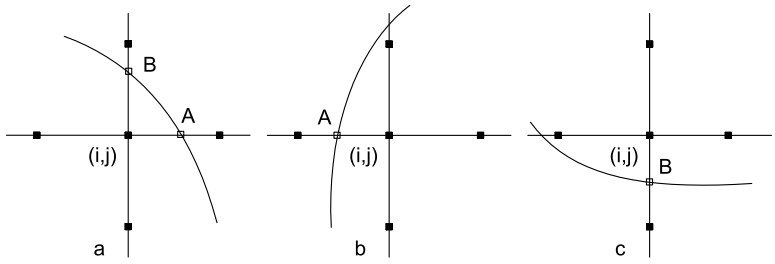

Fig. 4. Three typical situations for an interface crossing the mesh lines.

Scheme 1 is as follows:

$$u_{xx} = \frac{u_{i+1,j} - 2u_{i,j} + u_{i-1,j}}{\Delta x^2} + \text{sign}(\phi_{i,j}) \left(\frac{ax_\Gamma}{\Delta x^2} + \frac{bx_\Gamma \theta_x}{\Delta x} + \frac{[f]_A \theta_x^2}{2} \right), \tag{2.52}$$

$$u_{yy} = \frac{u_{i,j+1} - 2u_{i,j} + u_{i,j-1}}{\Delta y^2} + \text{sign}(\phi_{i,j}) \left(\frac{ay_\Gamma}{\Delta y^2} + \frac{by_\Gamma \theta_y}{\Delta y} + \frac{[f]_B \theta_y^2}{2} \right). \tag{2.53}$$

Scheme 2 is as follows:

$$\begin{aligned} u_{xx} = {} & \frac{1}{(1 + 2\theta_x - 2\theta_x^2)\Delta x^2} \big[(1 + 2\theta_x - \theta_x^2) u_{i-1,j} - (2 + 4\theta_x - \theta_x^2) u_{i,j} \\ & + (1 + \theta_x)^2 u_{i+1,j} - \theta_x^2 u_{i+2,j} + \text{sign}(\phi_{i,j})((1 + 2\theta_x) ax_\Gamma + (\theta_x + \theta_x^2) bx_\Gamma \Delta x) \big], \end{aligned} \tag{2.54}$$

$$\begin{aligned} u_{yy} = {} & \frac{1}{(1 + 2\theta_y - 2\theta_y^2)\Delta y^2} \big[(1 + 2\theta_y - \theta_y^2) u_{i,j-1} - (2 + 4\theta_y - \theta_y^2) u_{i,j} \\ & + (1 + \theta_y)^2 u_{i,j+1} - \theta_y^2 u_{i,j+2} + \text{sign}(\phi_{i,j})((1 + 2\theta_y) ay_\Gamma + (\theta_y + \theta_y^2) by_\Gamma \Delta y) \big]. \end{aligned} \tag{2.55}$$

Case b. Irregular point in *i*-direction.

Define

$$\theta_x = \frac{|\phi_{i-1,j}|}{|\phi_{i-1,j}| + |\phi_{i,j}|}, \tag{2.56}$$

then

$$ax_\Gamma = \theta_x a_{i,j} + (1 - \theta_x) a_{i-1,j}, \tag{2.57}$$

$$bx_\Gamma = \theta_x bx_{i,j} + (1 - \theta_x) bx_{i-1,j}. \tag{2.58}$$

Scheme 1 is as follows:

$$u_{xx} = \frac{u_{i+1,j} - 2u_{i,j} + u_{i-1,j}}{\Delta x^2} + \text{sign}(\phi_{i,j}) \left(\frac{ax_\Gamma}{\Delta x^2} - \frac{bx_\Gamma \theta_x}{\Delta x} + \frac{[f]_A \theta_x^2}{2} \right), \tag{2.59}$$

$$u_{yy} = \frac{1}{\Delta y^2}(u_{i,j+1} - 2u_{i,j} + u_{i,j-1}). \tag{2.60}$$

Scheme 2 is as follows:

$$\begin{aligned} u_{xx} = {} & \frac{1}{(1 + 2\theta_x - 2\theta_x^2)(\Delta x)^2} \big[(1 + 2\theta_x - \theta_x^2) u_{i+1,j} - (2 + 4\theta_x - \theta_x^2) u_{i,j} \\ & + (1 + \theta_x)^2 u_{i-1,j} - \theta_x^2 u_{i-2,j} + \text{sign}(\phi_{i,j})((1 + 2\theta_x) ax_\Gamma - (\theta_x + \theta_x^2) bx_\Gamma \Delta x) \big], \end{aligned} \tag{2.61}$$

$$u_{yy} = \frac{1}{\Delta y^2}(u_{i,j+1} - 2u_{i,j} + u_{i,j-1}). \tag{2.62}$$

Case c. Irregular point in *j*-direction.

Define

$$\theta_y = \frac{|\phi_{i,j-1}|}{|\phi_{i,j-1}| + |\phi_{i,j}|}, \tag{2.63}$$

then

$$ay_\Gamma = \theta_y a_{i,j} + (1-\theta_y)a_{i,j-1}, \tag{2.64}$$

$$by_\Gamma = \theta_y by_{i,j} + (1-\theta_y)by_{i,j-1}. \tag{2.65}$$

Scheme 1 is as follows:

$$u_{xx} = \frac{1}{\Delta x^2}(u_{i+1,j} - 2u_{i,j} + u_{i-1,j}), \tag{2.66}$$

$$u_{yy} = \frac{u_{i,j+1} - 2u_{i,j} + u_{i,j-1}}{\Delta y^2} + \text{sign}(\phi_{i,j})\left(\frac{ay_\Gamma}{\Delta y^2} - \frac{by_\Gamma \theta_y}{\Delta y} + \frac{[f]_B \theta_y^2}{2}\right). \tag{2.67}$$

Scheme 2 is as follows:

$$u_{xx} = \frac{1}{\Delta x^2}(u_{i+1,j} - 2u_{i,j} + u_{i-1,j}), \tag{2.68}$$

$$\begin{aligned} u_{yy} = {} & \frac{1}{(1+2\theta_y - 2\theta_y^2)\Delta y^2}\big[(1+2\theta_y - \theta_y^2)u_{i,j+1} - (2+4\theta_y - \theta_y^2)u_{i,j} \\ & + (1+\theta_y)^2 u_{i,j-1} - \theta_y^2 u_{i,j-2} + \text{sign}(\phi_{i,j})((1+2\theta_y)ay_\Gamma - (\theta_y + \theta_y^2)by_\Gamma \Delta y)\big]. \end{aligned} \tag{2.69}$$

Finally, combining the above expressions of u_{xx}, u_{yy} and (2.41) gives the finite difference scheme for irregular grid point (i, j).

It will be shown in Table 3 that both Scheme 1 and Scheme 2 are converge well for such 2D interface problems. Scheme 1 yields a linear system with a coefficient matrix just the same as that produced from standard discrete Laplace operator, so it is simpler than Scheme 2; but Scheme 2 performs is more effective than Scheme 1, and can be easily generalized to solve problems with variable coefficients.

2.4. The 2D Quasi-Poisson equation

Consider the 2D variable coefficient Poisson equation

$$(\beta u_x)_x + (\beta u_y)_y = f(x, y) \tag{2.70}$$

with interface jump conditions, $[u]_\Gamma = a(x, y)$ and $[\beta u_n]_\Gamma = b(x, y)$.

In order to apply the IMIB method in a grid direction, it is necessary to derive interface jump conditions for u_x or u_y only. Differentiating interface jump condition $[u]_\Gamma = a$ along the tangential direction of the interface, we obtain

$$[u_\tau]_\Gamma = a_\tau \tag{2.71}$$

where u_τ is the derivative in the tangential direction $\vec{\tau} = (-n_2, n_1)$. Considering these relations, the interface jump conditions can be reformulated as

$$[u_\tau]_\Gamma = -[u_x]_\Gamma n_2 + [u_y]_\Gamma n_1 = a_\tau, \tag{2.72}$$

$$[\beta u_n]_\Gamma = [\beta u_x]_\Gamma n_1 + [\beta u_y]_\Gamma n_2 = b. \tag{2.73}$$

Then, combining (2.72) multiplied by $-n_2$ with (2.73) multiplied by n_1 gives

$$[\tilde{\beta} u_x]_\Gamma = bx \tag{2.74}$$

where

$$\tilde{\beta} = \beta n_1^2 + n_2^2, \tag{2.75}$$

$$bx = bn_1 - a_\tau n_2 - [(\beta - 1)n_1 n_2 u_y]. \tag{2.76}$$

For finite difference approximation of derivatives with respect to x at an irregular point, the jump condition (2.74) is used. And u_y on the right-hand side of (2.76) is evaluated by one-sided second-order difference formulas. Similarly, for finite difference approximation of derivatives with respect to y, the following jump condition is used:

$$[\tilde{\beta} u_y]_\Gamma = by \tag{2.77}$$

where

$$\tilde{\beta} = \beta n_2^2 + n_1^2, \tag{2.78}$$

$$by = bn_2 + a_\tau n_1 - [(\beta - 1)n_1 n_2 u_x]. \tag{2.79}$$

Again, the partial derivative u_x on the right-hand side of (2.79) is evaluated by one-sided second-order difference formulas.

A straightforward extension of the 2D discretization will enable us to solve 3D elliptic interface problems.

3. Convergence analysis

3.1. Preliminaries

Let us first introduce some notations. Given h as a parameter(e.g., h is the maximum mesh size), two finite and mutually disjoint sets of mesh points are constructed. One of these sets, called Ω^h, consists of points in Ω, and the other one consists points of $\partial\Omega$ called $\partial\Omega^h$. For convenience, we denote $\bar{\Omega}^h = \Omega^h \cup \partial\Omega^h$.

For simplicity, we assume that the discrete scheme for the approximation solution of (1.1) and (1.2) with the Dirichlet boundary condition $u(\mathbf{x})|_{\partial\Omega} = g(\mathbf{x})$ is of the form

$$L_h u(P) = f^h(P) + a^h(\Gamma, P) + b^h(\Gamma, P), \quad P \in \Omega^h \tag{3.1}$$

$$u(P) = g^h(P), \quad P \in \partial\Omega^h \tag{3.2}$$

where $a^h(\Gamma, P)$ and $b^h(\Gamma, P)$ are "approximations" to the jump condition (1.2).

Since u is usually piecewise smooth in Ω, the points in Ω^h may be subdivided into $k(k \geq 1)$ mutually disjoint subsets $\{\Omega_i^h\}_{i=1}^k$, with k independent of h, depending upon the order of approximation, i.e.,

$$\left|L_h u^h(P) - L_h u(P)\right| \leq K_i h^{\alpha_i}, \quad \forall P \in \Omega_i^h,\ 1 \leq i \leq k, \tag{3.3}$$

the constants K_i, as well as the exponents $\alpha_i \geq 0$, depending upon the smoothness of u, but independent of h.

To prove the convergence of our method, we first give the following lemma which is a generalization of Theorem 5 of [38] for elliptic interface problems.

Lemma 3.1. *Assume that the operator L_h satisfies the discrete maximum principle* [38]*, and truncation error estimate* (3.3) *holds. Furthermore, for each $i(1 \leq i \leq k)$ and h, there exists a function w^h such that (letting $\|u\|_{\bar{\Omega}^h} = \sup\{|u(x)|; x \in \bar{\Omega}^h\}$)*

$$L_h w^h(P) \geq h^{-\beta_i}, \quad P \in \Omega_i^h$$
$$L_h w^h(P) \geq 0, \quad P \in \Omega_j^h,\ j \neq i,\ 1 \leq j \leq k$$
$$w^h(P) \geq 0, \quad P \in \bar{\Omega}^h,$$
$$\|w^h\|_{\bar{\Omega}^h} \leq H_i.$$

Then the global error of the approximation solution u^h from (3.1) *and* (3.2) *is bounded by*

$$\|u - u^h\|_{\bar{\Omega}^h} \leq \sum_{i=1}^{k} K_i H_i h^{\alpha_i+\beta_i} \leq C h^{\min\{\alpha_i+\beta_i;\, 1\leq i\leq k\}}$$

for some constant C, depending only upon the constants K_i and H_i.

3.2. One-dimensional problems

Consider the 1D elliptic model problem

$$(\beta u_x)_x = f(x), \quad 0 < x < 1, \tag{3.4}$$
$$u(0) = u_0, \qquad u(1) = u_1,$$

with jump conditions

$$[u_x]_{x=\alpha} = a_\Gamma, \qquad [\beta u_x]_{x=\alpha} = b_\Gamma, \tag{3.5}$$

where α is the exact interface location. Without loss of generality, we assume that $\beta = \beta^-$ if $x < \alpha$ and $\beta = \beta^+$ if $x > \alpha$, and denote $\max\{\beta^+, \beta^-\}$, $\min\{\beta^+, \beta^-\}$, β^+/β^- and $\max\{\beta^+/\beta^-, \beta^-/\beta^+\}$ by $\beta_{\max}$, $\beta_{\min}$, r and $r_{\max}$, respectively.

We can then give the error estimate for the above model problem as stated in the following theorem:

Theorem 3.2. *Let $u(x)$ be the exact solution to* (3.4) *and* (3.5)*. Assume $u(x)$ is piecewisely continuous at least until fourth order. Then we have the following error estimate for the approximation solution u^h*

$$\|u - u^h\|_{\bar{\Omega}^h} \leq \left\{ \frac{M_{xxxx} r_{\max}}{24} \max\{\alpha^2, (1-\alpha)^2\} + \frac{M_{xxx}(2 + r_{\max})\beta_{\max}}{6} \max\left\{ \frac{\alpha}{\beta^-}, \frac{1-\alpha}{\beta^+} \right\} \right\} h^2$$

where

$$M_{xxx} = \max\left\{ \sup_{0<x<\alpha} |u'''(x)|, \sup_{\alpha<x<1} |u'''(x)| \right\},$$
$$M_{xxxx} = \max\left\{ \sup_{0<x<\alpha} |u''''(x)|, \sup_{\alpha<x<1} |u''''(x)| \right\}.$$

Proof 3.3. Without loss of generality, we assume $x_k \le \alpha \le x_{k+1}$ with a uniform grid, $x_i = ih$, $i = 0, 1, \ldots, n+1$ where $h = 1/(n+1)$. From Section 2.2, we know that the operator L_h is defined by:

$$(L_h u^h)_i = -\left[\beta_{i+1/2}\left(\frac{u_{i+1}-u_i}{h}\right) - \beta_{i-1/2}\left(\frac{u_i - u_{i-1}}{h}\right)\right]\Big/ h \tag{3.6}$$

where

$$\beta_{i+1/2} = \begin{cases} \beta^-, & i < k, \\ \hat{\beta}, & i = k, \\ \beta^+, & i > k. \end{cases} \tag{3.7}$$

Obviously, the difference operator L_h satisfies the discrete maximum principle from Theorem 3 in [38]. Using the jump conditions and Taylor expansions of $u_{k-1}, u_k, u_{k+1}, u_{k+2}$ at the interface, we obtain

$$\begin{aligned} \left|L_h u^h(x_k) - L_h u(x_k)\right| &= \left|\frac{\hat{\beta}(1-\theta)(r+\theta+\theta^2-3r\theta^2)h}{6}u^-_{xxx} + \frac{\hat{\beta}(1-\theta)^3 h}{3}u^+_{xxx} + O(h^2)\right| \\ &\le \left(\frac{|1/r+\theta+\theta^2-3\theta^2/r|(1-\theta)}{6} + \frac{(1-\theta)^3}{3}\right)M_{xxx}\hat{\beta}h + O(h^2) \\ &< \frac{(2+r_{\max})\beta_{\max}}{6}M_{xxx}h + O(h^2) \\ \left|L_h u^h(x_{k+1}) - L_h u(x_{k+1})\right| &= \left|\frac{\hat{\beta}\theta^3 h}{3}u^-_{xxx} + \frac{\hat{\beta}((1-3r)\theta^2+(6r-3)\theta+2-2r)\theta^2 h}{6}u^+_{xxx} + O(h^2)\right| \\ &\le \left(\frac{\theta^3}{3} + \frac{|(1-3r)\theta^2+(6r-3)\theta+2-2r|\theta^2}{6}\right)M_{xxx}\hat{\beta}h + O(h^2) \\ &< \frac{(2+r_{\max})\beta_{\max}}{6}M_{xxx}h + O(h^2). \end{aligned}$$

Thus, we have the following truncation error estimate:

$$\left|L_h u^h(P) - L_h u(P)\right| \le \frac{(2+r_{\max})\beta_{\max}}{6}M_{xxx}h, \quad P \in \Omega_1^h = \{x_k\} \cup \{x_{k+1}\}, \tag{3.8}$$

$$\left|L_h u^h(P) - L_h u(P)\right| = \frac{\beta_{\max}}{12}M_{xxxx}h^2 + O(h^4), \quad P \in \Omega_2^h = \cup_{i=1}^n \{x_i\} \setminus \Omega_1^h. \tag{3.9}$$

Now, we introduce the functions w_1^h and w_2^h defined as follows:

$$w_1^h(x_i) = \frac{i}{k}\cdot E_1, \quad 0 \le i \le k, \tag{3.10}$$

$$w_1^h(x_i) = \frac{n+1-i}{n-k}\cdot E_2, \quad k+1 \le i \le n+1 \tag{3.11}$$

and

$$w_2^h(x_i) = \frac{1}{\beta_{\min}}\left(\frac{\max\{\alpha^2, (1-\alpha)^2\}}{2} - \frac{1}{2}(x_i-\alpha)^2\right), \quad 1 \le i \le n+1, \tag{3.12}$$

where

$$E_1 = \frac{\alpha(2\hat{\beta}(1-\alpha)+\beta^+ h)}{\hat{\beta}(\beta^+\alpha+\beta^-(1-\alpha))+\beta^+\beta^- h} \tag{3.13}$$

$$E_2 = \frac{(1-\alpha)(2\hat{\beta}\alpha+\beta^- h)}{\hat{\beta}(\beta^+\alpha+\beta^-(1-\alpha))+\beta^+\beta^- h} \tag{3.14}$$

are the solutions of

$$\begin{bmatrix} -\hat{\beta} & \hat{\beta}+\beta^+\dfrac{h}{1-\alpha} \\ \hat{\beta}+\beta^-\dfrac{h}{\alpha} & -\hat{\beta} \end{bmatrix}\cdot\begin{bmatrix} E_1 \\ E_2 \end{bmatrix} = \begin{bmatrix} h \\ h \end{bmatrix}. \tag{3.15}$$

Then a simple computation shows that

$$L_h w_1^h(P) = 0, \quad P \in \Omega_2^h, \tag{3.16}$$

$$L_h w_2^h(P) \geq 0, \quad P \in \Omega_1^h, \tag{3.17}$$

$$L_h w_2^h(P) \geq 1, \quad P \in \Omega_2^h. \tag{3.18}$$

To obtain the upper bound for $\|w_1^h\|_{\bar{\Omega}^h}$, we discuss it in two different cases:

Case 1. $\alpha \leq \frac{\beta^-}{\beta^+ + \beta^-}$

$$E_1 \leq E_2 \leq \frac{(1-\alpha)(2\hat{\beta}\alpha + \beta^- h)}{\hat{\beta}(2\beta^+\alpha) + \beta^+\beta^- h} \leq \frac{1-\alpha}{\beta^+}.$$

Case 2. $\alpha > \frac{\beta^-}{\beta^+ + \beta^-}$

$$E_2 \leq E_1 \leq \frac{\alpha(2\hat{\beta}(1-\alpha) + \beta^+ h)}{\hat{\beta}(2\beta^-(1-\alpha)) + \beta^+\beta^- h} \leq \frac{\alpha}{\beta^-}.$$

Thus we have

$$\|w_1^h\|_{\bar{\Omega}^h} = \max\{E_1, E_2\} \leq \max\left\{\frac{\alpha}{\beta^-}, \frac{1-\alpha}{\beta^+}\right\}. \tag{3.19}$$

Noticing that $kh + \theta h = \alpha$, $(n-k)h + (1-\theta)h = 1-\alpha$, we can obtain

$$\frac{1}{k} = \frac{h}{\alpha - \theta h} \geq \frac{h}{\alpha}, \tag{3.20}$$

$$\frac{1}{n-k} = \frac{h}{1-\alpha-(1-\theta)h} \geq \frac{h}{1-\alpha}. \tag{3.21}$$

Then, substituting (3.10) and (3.11) into (3.6) gives

$$\begin{aligned} L_h w_1^h(x_k) &= -\frac{\hat{\beta}(E_2 - E_1) - \beta^- E_1/k}{h^2} \\ &= \frac{1}{h^2}\left(\left(\hat{\beta} + \frac{\beta^-}{k}\right)E_1 - \hat{\beta}E_2\right) \\ &\geq \frac{1}{h^2}\left(\left(\hat{\beta} + \frac{\beta^- h}{\alpha}\right)E_1 - \hat{\beta}E_2\right) \\ &= h^{-1} \end{aligned} \tag{3.22}$$

and

$$\begin{aligned} L_h w_1^h(x_{k+1}) &= -\frac{-\beta^+ E_2/(n-k) - \hat{\beta}(E_2 - E_1)}{h^2} \\ &= \frac{1}{h^2}\left(-\hat{\beta}E_1 + \left(\hat{\beta} + \frac{\beta^+}{n-k}\right)E_2\right) \\ &\geq \frac{1}{h^2}\left(-\hat{\beta}E_1 + \left(\hat{\beta} + \frac{\beta^+ h}{1-\alpha}\right)E_2\right) \\ &= h^{-1}. \end{aligned} \tag{3.23}$$

Since $w_1^h \geq 0$, and $w_2^h \geq 0$, $\|w_2^h\|_{\bar{\Omega}^h} \leq \frac{\max\{\alpha^2, (1-\alpha)^2\}}{2\beta_{\min}}$, we may conclude that

$$\|u - u^h\|_{\bar{\Omega}^h} \leq \left\{\frac{M_{xxxx} r_{\max}}{24}\max\{\alpha^2, (1-\alpha)^2\} + \frac{M_{xxx}(2 + r_{\max})\beta_{\max}}{6}\max\left\{\frac{\alpha}{\beta^-}, \frac{1-\alpha}{\beta^+}\right\}\right\} h^2.$$

from Lemma 3.1. □

Remark 3.4. In the particular case when $\beta^+ = \beta^- \equiv 1$, set $w_2^h(x_i) = \frac{1}{8} - \frac{1}{2}(x_i - \frac{1}{2})^2$ in place of (3.12), we can obtain the following simple error estimate:

$$\|u - u^h\|_{\bar{\Omega}^h} \leq \left\{\frac{1}{96}M_{xxxx} + \frac{\max\{\alpha, 1-\alpha\}}{2}M_{xxx}\right\} h^2.$$

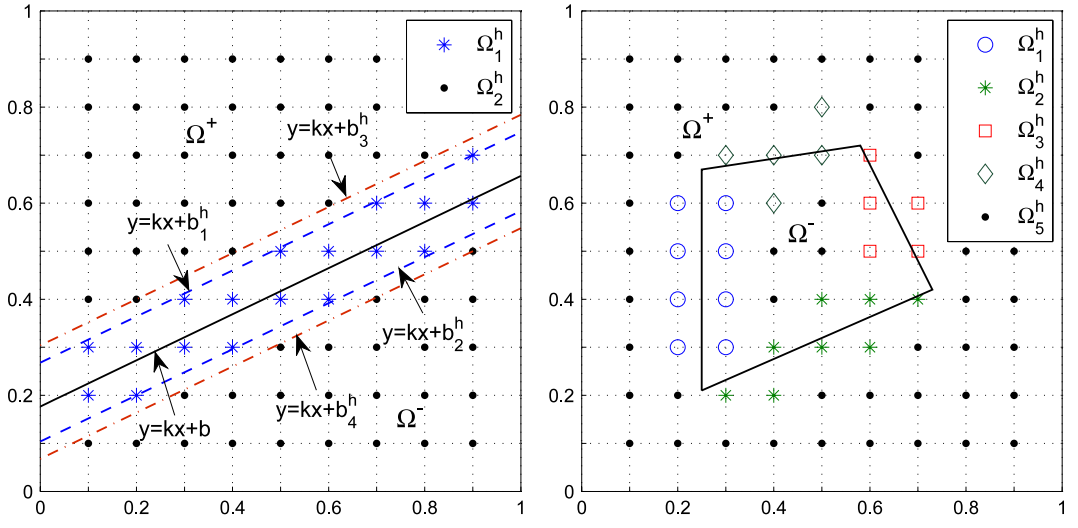

(a) Straight line. (b) Polygon.

Fig. 5. Computational domains with different interfaces.

3.3. Two-dimensional problems

We begin with the Poisson equation with singular sources. Consider the 2D elliptic model problem

$$u_{xx} + u_{yy} = f(x, y) \tag{3.24}$$

with interface jump conditions, $[u]_\Gamma = a(x, y)$ and $[u_n]_\Gamma = b(x, y)$.

To construct comparison functions, we first consider the case when the interface in domain $[0, 1] \times [0, 1]$ is a straight line $y = kx + b$ for simplicity. As shown in Fig. 5(a), the straight line $y = kx + b_1^h$ parallel to the interface, passes the farthest irregular point A from the interface in Ω^+; the straight line $y = kx + b_2^h$ parallel to the interface, passes the nearest regular point B from the interface in Ω^+. The straight lines $y = kx + b_3^h$ and $y = kx + b_4^h$ are determined similarly in Ω^-.

We define d_h^* to be the distance

$$d_h^* = \min\{b_3^h - b_1^h, b_2^h - b_4^h\}, \tag{3.25}$$

and assume that there exists a constant $\delta > 0$, such that the inequality

$$d_h^* \geq \delta h \tag{3.26}$$

holds for all h. When the interface is parallel to one of the axes, δ can be set to 1. Then, we can obtain the following lemma for the construction of comparison functions:

Lemma 3.5. *There exist nonnegative and bounded functions w_1^h and w_2^h such that*

$$\begin{aligned} &L_h w_1^h(P) \geq 1/h, \quad P \in \Omega_1^h, \\ &L_h w_1^h(P) \geq 0, \quad P \in \Omega_2^h, \\ &L_h w_2^h(P) \geq 1, \quad P \in \Omega_h = \Omega_1^h \cup \Omega_2^h, \end{aligned}$$

where Ω_1^h and Ω_2^h denote collections of irregular grid points and regular grid points in domain $[0, 1] \times [0, 1]$ with interface defined by straight line $y = kx + b$.

Proof 3.6. We know that the operator L_h is defined by

$$(L_h u^h)_{i,j} = -\left(\frac{u_{i+1,j} - 2u_{i,j} + u_{i-1,j}}{h} + \frac{u_{i,j+1} - 2u_{i,j} + u_{i,j-1}}{h}\right) \Big/ h \tag{3.27}$$

from (2.52) and (2.53). Now, we introduce the functions w_1^h and w_2^h defined as follows:

$$w_1^h(x_i, y_j) = \tilde{w}_1^h(y_j - kx_i - b) \triangleq \tilde{w}_1^h(\xi_{i,j}) = \begin{cases} E, & b_2^h - b \leq \xi_{i,j} \leq b_1^h - b, \\ E - \dfrac{\xi_{i,j} - (b_1^h - b)}{\delta}, & \xi_{i,j} > b_1^h - b, \\ E - \dfrac{(b_2^h - b) - \xi_{i,j}}{\delta}, & \xi_{i,j} < b_2^h - b, \end{cases}$$

and

$$w_2^h(x_i, y_j) = \frac{1 - x_i^2}{2} \tag{3.28}$$

where E is a positive constant that makes $w_1^h \geq 0$. From the definition of w_1^h (3.6) and (3.26), it follows that

$$w_1^h(P) \leq E - h, \quad P \in \Omega_2^h. \tag{3.29}$$

Thus, we have

$$L_h w_1^h(P) \geq \frac{-E + 2E - (E - h)}{h^2} = \frac{1}{h}, \quad P \in \Omega_1^h. \tag{3.30}$$

A simple computation shows that

$$L_h w_1^h(P) = 0, \quad P \in \Omega_2^h, \tag{3.31}$$

$$L_h w_2^h(P) \geq 1, \quad P \in \Omega^h, \tag{3.32}$$

which is what we were to prove. □

Now, we can use Lemmas 3.1 and 3.5 to prove the following convergence theorem.

Theorem 3.7. *Let $u(x, y)$ be the exact solution to (3.24) in the 2D domain $[0, 1] \times [0, 1]$ with general interface. Assuming $u(x, y)$ has piecewisely until fourth-order continuous derivatives, then we have the following error estimate for the approximation solution u^h*

$$\|u - u^h\|_{\bar{\Omega}^h} \leq C \cdot h^2$$

where C is a constant independent of h.

Proof 3.8. Since arbitrarily closed curve (the interface Γ) can be approximated by a polygon, we can assume that the interface in computational domain is a quadrangle as shown in Fig. 5(b). We know that the operator L_h is defined by

$$(L_h u^h)_{i,j} = -\left(\frac{u_{i+1,j} - 2u_{i,j} + u_{i-1,j}}{h} + \frac{u_{i,j+1} - 2u_{i,j} + u_{i,j-1}}{h}\right) \Big/ h \tag{3.33}$$

from (2.52) and (2.53). It is easy to verify that the above difference operator L_h satisfies the discrete maximum principle from Theorem 3 in [38]. By virtue of the jump conditions and Taylor expansions technique, we can obtain the following truncation error estimate:

$$\left|L_h u^h(P) - L_h u(P)\right| \leq K_i h, \quad P \in \Omega_i^h, 1 \leq i \leq 4 \tag{3.34}$$

$$\left|L_h u^h(P) - L_h u(P)\right| \leq K_5 h^2, \quad P \in \Omega_5^h \tag{3.35}$$

where Ω_5^h is the collection of regular grid points, and $\Omega_i^h (1 \leq i \leq 4)$ are the collection of irregular grid points near ith edge of the quadrangle respectively; see Fig. 5(b). With Lemma 3.5, we can introduce comparison functions $w_i^h (1 \leq i \leq 5)$ such that

$$L_h w_i^h(P) \geq 1/h, \quad P \in \Omega_i^h, 1 \leq i \leq 4 \tag{3.36}$$

$$L_h w_i^h(P) \geq 0, \quad P \in \Omega_j^h, j \neq i, 1 \leq j \leq 5. \tag{3.37}$$

$$L_h w_5^h(P) \geq 1, \quad P \in \Omega^h. \tag{3.38}$$

Then, we may conclude that

$$\|u - u^h\|_{\bar{\Omega}^h} \leq Ch^2$$

from Lemma 3.1. □

The convergence analysis of the IMIB method applied to 2D interface problems with variable coefficients is under our consideration.

4. Numerical examples

In this section, we examine the performance of the IMIB method for 2D elliptic interface problems by considering several case studies with different boundary and interface geometry. The tests confirm the expected second-order accuracy for the

Table 2
Numerical convergence test for Example 4.1.

n	GFM		IIM		IMIB	
	L_∞	Order	L_∞	Order	L_∞	Order
10	1.07(−2)		5.71(−4)		2.42(−4)	
40	2.70(−3)	0.99	3.66(−5)	1.98	1.13(−5)	2.21
160	6.91(−4)	0.98	2.30(−6)	2.00	6.40(−7)	2.07
640	1.73(−4)	1.00	1.44(−7)	2.00	3.90(−8)	2.02
2560	4.32(−5)	1.00	8.99(−9)	2.00	2.42(−9)	2.01

proposed method. Preconditioned conjugate gradient method (PCG) with the preconditioner being the diagonal part of the discrete matrix is adopted to solve symmetric positive-definite linear systems obtained from IMIB discretizations; UMFPACK is used to solve unsymmetric cases.

In this section, the numerical errors of the computations are measured in the L_∞ norm

$$\|E_n\|_\infty = \max_{i,j} |u_{i,j} - u^h_{i,j}|$$

and the discrete L_2 norm

$$\|E_n\|_2 = \sqrt{\frac{1}{n_x \cdot n_y} \sum_{i=1}^{n_x} \sum_{j=1}^{n_y} (u_{i,j} - u^h_{i,j})^2}$$

given an exact solution $u_{i,j}$ and an approximation solution $u^h_{i,j}$. Here, n_x and n_y are the numbers of grid points in x- and y-directions, respectively. The order of convergence is computed from

$$\text{order} = \frac{\log\left(\|E_{n_1}\|/\|E_{n_2}\|\right)}{\log\left(n_2/n_1\right)}$$

which is the solution of the equation

$$\|E_n\| = Ch^{\text{order}}$$

with two different n's.

Example 4.1. Consider $(\beta u_x)_x = f(x)$ on $[0, 1]$ with one interface at $x = 1/3$ where $\beta = 1$ if $x \le 1/3$ and $\beta = 10$ if $x > 1/3$. Dirichlet boundary condition, as well as the jump conditions $[u]$ and $[\beta u_x]$ along the interface are determined from the exact solution

$$u(x) = \begin{cases} x^2, & x \le 1/3, \\ e^x, & x > 1/3. \end{cases}$$

Table 2 shows the results of the numerical accuracy tests. It is easily seen that the GFM converges with first-order accuracy, while the IIM and IMIB methods converge well with second-order accuracy in the sense of L_∞-norm. And we also see that the results of the IMIB (columns 6, 7) method are more accurate than those of the IIM (columns 4, 5).

Example 4.2. This example is taken from [12]. Consider $\Delta u = 0$ in 2D domain $[-1, 1] \times [-1, 1]$ with the interface defined by circle $x^2 + y^2 = 0.5^2$ with an outward normal vector, $\vec{n} = (2x, 2y)$. Dirichlet boundary condition, as well as the jump conditions $[u]$ and $[u_n]$ along the interface are determined from the exact solution

$$u(x, y) = \begin{cases} 1, & r \le 0.5, \\ 1 + \ln(2r), & r > 0.5, \end{cases}$$

where $r = \sqrt{x^2 + y^2}$. Fig. 6 shows the numerical solution with 61 grid points in each direction and Table 3 shows the results of the numerical accuracy tests.

Example 4.3. This example is taken from [26]. Consider $\nabla \cdot (\beta \nabla u) = f(x, y)$ in 2D domain $[-1, 1] \times [-1, 1]$ with a circular interface $x^2 + y^2 = 0.5^2$ inside. Dirichlet boundary condition, as well as the jump conditions $[u]$ and $[u_n]$ along the interface are determined from the exact solution

$$u(x, y) = \begin{cases} r^2, & r \le 0.5, \\ \dfrac{1}{4}\left(1 - \dfrac{1}{8b} - \dfrac{1}{b}\right) + \left(\dfrac{r^4}{2} + r^2\right) \Big/ b, & r > 0.5, \end{cases}$$

with the diffusion coefficient

$$\beta(x, y) = \begin{cases} 2, & r \le 0.5, \\ b, & r > 0.5. \end{cases}$$

Table 3
Numerical convergence test for Example 4.2.

$n_x \times n_y$	Scheme 1				Scheme 2			
	L_∞	Order	L_2	Order	L_∞	Order	L_2	Order
20 × 20	3.3(−2)		1.5(−2)		7.3(−3)		3.9(−3)	
40 × 40	1.3(−2)	1.35	5.4(−3)	1.47	1.9(−3)	1.94	9.2(−4)	2.08
80 × 80	4.9(−3)	1.40	1.9(−3)	1.51	4.1(−4)	2.21	1.6(−4)	2.50
160 × 160	1.9(−3)	1.37	6.8(−4)	1.47	9.9(−5)	2.05	3.9(−5)	2.07
320 × 320	7.1(−4)	1.43	2.4(−4)	1.50	2.2(−5)	2.16	8.1(−6)	2.26
640 × 640	2.6(−4)	1.42	8.5(−5)	1.50	4.4(−6)	2.32	1.4(−6)	2.54

Table 4
Numerical convergence test for Example 4.3.

$n_x \times n_y$	L_∞	Order	L_2	Order
20 × 20	6.47(−4)		3.70(−3)	
40 × 40	1.89(−4)	1.77	9.00(−4)	2.04
80 × 80	5.07(−5)	1.90	1.61(−4)	2.49
160 × 160	1.25(−5)	2.02	3.85(−5)	2.06
320 × 320	3.11(−6)	2.00	8.07(−6)	2.26
640 × 640	7.98(−7)	1.96	1.39(−6)	2.54

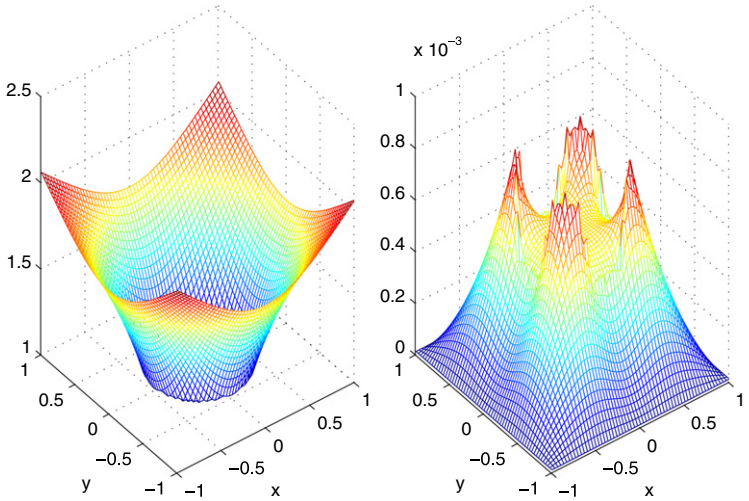

Fig. 6. The computed solution (left) and error (right) for Example 4.2.

The source term can be determined accordingly:

$$f(x, y) = \begin{cases} 8, & (x, y) \in \Omega^-, \\ 8r^2 + 4, & (x, y) \in \Omega^+. \end{cases}$$

Fig. 7 shows the numerical solution with 61 grid points in each direction and Table 4 shows the results of the numerical accuracy tests.

Example 4.4. This example is taken from [12]. Consider $\Delta u = 0$ in 2D domain $[-1, 1] \times [-1, 1]$ with the interface defined by circle $x^2 + y^2 = 0.5^2$ with an outward normal vector, $\vec{n} = (2x, 2y)$. Dirichlet boundary condition, as well as the jump conditions $[u]$ and $[u_n]$ along the interface are determined from the exact solution

$$u(x, y) = \begin{cases} e^x \cos y, & r \le 0.5, \\ 0, & r > 0.5, \end{cases}$$

where $r = \sqrt{x^2 + y^2}$. Fig. 8 shows the numerical solution with 61 grid points in each direction and Table 5 shows the results of the numerical accuracy tests.

Example 4.5. This example is taken from [12]. Consider $\Delta u = 0$ in 2D domain $[-1, 1] \times [-1, 1]$ with the interface defined by circle $x^2 + y^2 = 0.5^2$ with an outward normal vector, $\vec{n} = (2x, 2y)$. Dirichlet boundary condition, as well as the jump

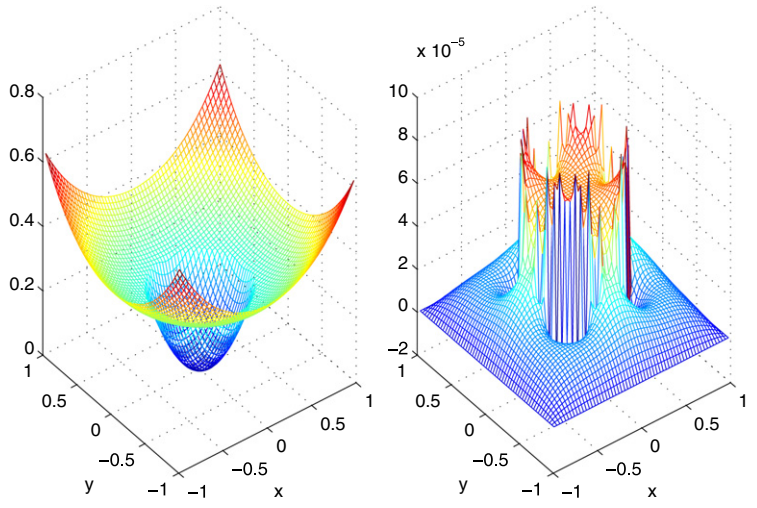

Fig. 7. The computed solution (left) and error (right) for Example 4.3 with $b = 10$.

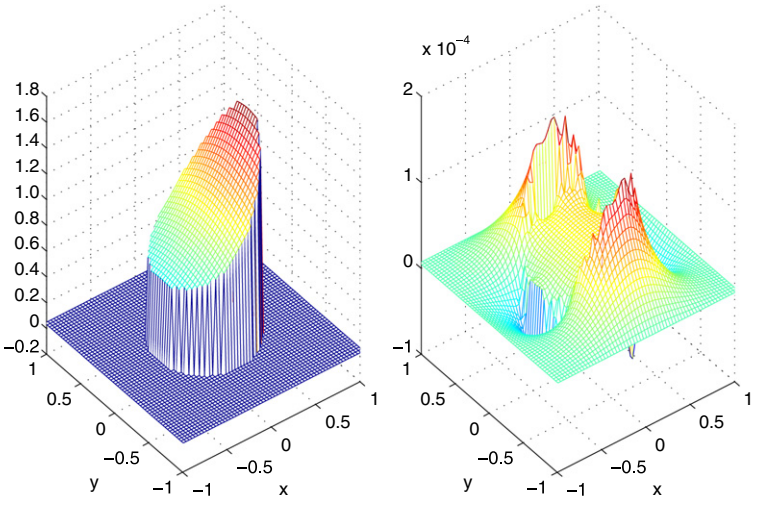

Fig. 8. The computed solution (left) and error (right) for Example 4.4.

Table 5
Numerical convergence test for Example 4.4.

$n_x \times n_y$	L_∞	Order	L_2	Order
20×20	9.76(−4)		2.69(−4)	
40×40	3.06(−4)	1.67	7.72(−5)	1.80
80×80	8.18(−5)	1.90	2.17(−5)	1.83
160×160	2.44(−5)	1.75	5.66(−6)	1.94
320×320	6.95(−6)	1.81	1.35(−6)	2.06
640×640	1.43(−6)	2.28	3.17(−7)	2.09

conditions $[u]$ and $[u_n]$ along the interface are determined from the exact solution

$$u(x, y) = \begin{cases} x^2 - y^2, & r \le 0.5, \\ 0, & r > 0.5, \end{cases}$$

where $r = \sqrt{x^2 + y^2}$. Fig. 9 shows the numerical solution with 61 grid points in each direction and Table 6 shows the results of the numerical accuracy tests.

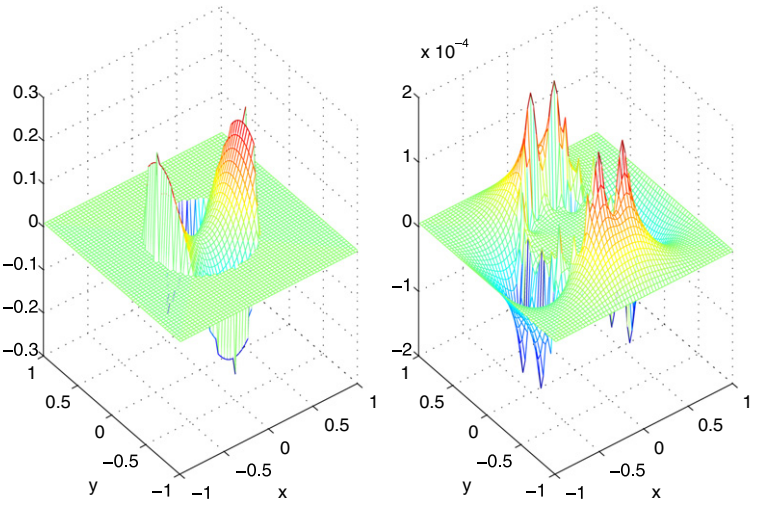

Fig. 9. The computed solution (left) and error (right) for Example 4.5.

Table 6
Numerical convergence test for Example 4.5.

$n_x \times n_y$	L_∞	Order	L_2	Order
20×20	1.82(−3)		6.74(−4)	
40×40	4.51(−4)	2.02	1.03(−4)	2.71
80×80	1.19(−4)	1.92	2.33(−5)	2.15
160×160	3.18(−5)	1.91	7.02(−6)	1.73
320×320	8.40(−6)	1.92	1.51(−6)	2.21
640×640	2.27(−6)	1.89	3.69(−7)	2.03

Table 7
Numerical convergence test for Example 4.6.

$n_x \times n_y$	L_∞	Order	L_2	Order
24×24	1.69(−3)		5.71(−4)	
58×58	3.22(−4)	1.88	1.00(−4)	1.97
88×88	1.37(−4)	2.05	3.98(−5)	2.22
157×157	4.37(−5)	1.97	1.37(−5)	1.84
320×320	1.05(−5)	2.01	3.09(−6)	2.09
640×640	2.69(−6)	1.96	7.95(−7)	1.96

Example 4.6. This example is taken from [15]. Consider $\nabla \cdot (\beta \nabla u) = f(x, y)$ in 2D domain $[-1, 1] \times [-1, 1]$ with the interface determined by

$$\begin{cases} x(\theta) = 0.02\sqrt{5} + (0.5 + 0.2\sin(5\theta))\cos\theta, \\ y(\theta) = 0.02\sqrt{5} + (0.5 + 0.2\sin(5\theta))\sin\theta, \end{cases} \quad 0 \le \theta < 2\pi$$

where $\beta = 1$ in Ω^- and $\beta = 10$ in Ω^+. Dirichlet boundary condition, as well as the jump conditions $[u]$ and $[\beta u_n]$ along the interface are determined from the exact solution

$$u(x, y) = \begin{cases} \dfrac{r^2}{\beta^-}, & (x, y) \in \Omega^-, \\ \dfrac{r^4 - 0.1\ln(2r)}{\beta^+}, & (x, y) \in \Omega^+, \end{cases}$$

where $r = \sqrt{x^2 + y^2}$. The source term can be determined accordingly:

$$f(x, y) = \begin{cases} 4, & (x, y) \in \Omega^-, \\ 16r^2, & (x, y) \in \Omega^+. \end{cases}$$

Fig. 10 shows the numerical solution with 59 grid points in each direction and Table 7 shows the results of the numerical accuracy tests.

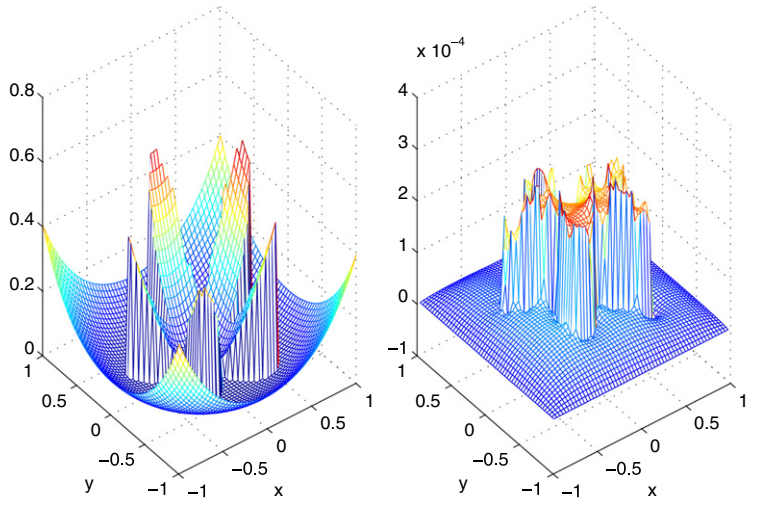

Fig. 10. The computed solution (left) and error (right) for Example 4.6.

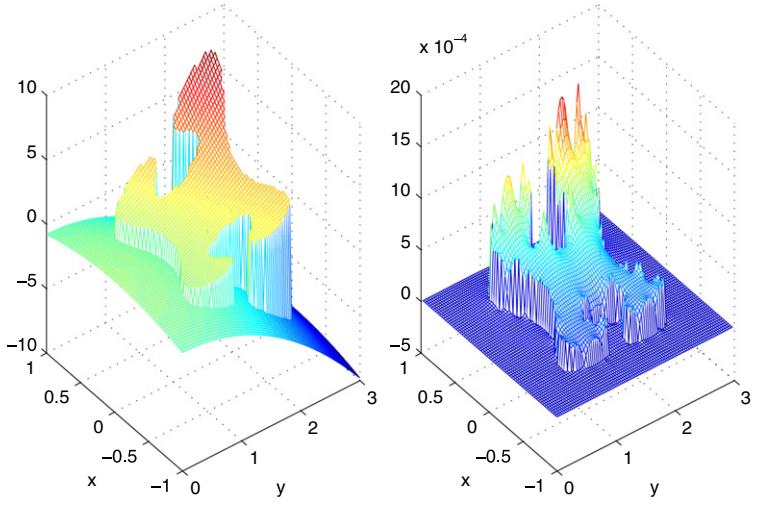

Fig. 11. The computed solution (left) and error (right) for Example 4.7.

Example 4.7. This example is taken from [27]. Consider $\nabla \cdot (\beta \nabla u) = f(x, y)$ in 2D domain $[-1, 1] \times [0, 3]$ with a jigsaw puzzle like interface given below

$$\begin{cases} x(\theta) = 0.6\cos\theta - 0.3\cos(3\theta) \\ y(\theta) = 1.5 + 0.7\sin\theta - 0.07\sin(3\theta) + 0.2\sin(7\theta) \end{cases} \quad 0 \le \theta < 2\pi$$

where $\beta = 1$ in Ω^- and $\beta = 10$ in Ω^+. Dirichlet boundary condition, as well as the jump conditions $[u]$ and $[\beta u_n]$ along the interface are determined from the exact solution

$$u(x, y) = \begin{cases} e^x(x^2 \sin y + y^2), & (x, y) \in \Omega^-, \\ -(x^2 + y^2), & (x, y) \in \Omega^+, \end{cases}$$

where $r = \sqrt{x^2 + y^2}$. The source term can be determined accordingly:

$$f(x, y) = \begin{cases} e^x(2 + y^2 + 2\sin y + 4x\sin y)\beta^-, & (x, y) \in \Omega^-, \\ -4\beta^+, & (x, y) \in \Omega^+. \end{cases}$$

Fig. 11 shows the numerical solution with 67 grid points in the x-direction and 100 grid points in the y-direction. Table 8 shows the results of the numerical accuracy tests.

Table 8
Numerical convergence test for Example 4.7.

$n_x \times n_y$	L_∞	Order	L_2	Order
38×57	4.24(−3)		8.23(−4)	
66×99	1.67(−3)	1.69	2.80(−4)	1.95
118×177	5.68(−4)	1.85	8.87(−5)	1.98
204×306	2.05(−4)	1.86	3.29(−5)	1.81
410×615	5.30(−5)	1.94	6.94(−6)	2.23

5. Conclusion

An IMIB method with second-order accuracy is presented for elliptic interface problems on Cartesian grids in this paper. The original MIB method is of arbitrarily high order in principle as the jump conditions are iteratively used. However, till now there is no theoretical proof of convergence of the MIB method for elliptic interface problems. The IMIB method we propose here is simple and of second-order accuracy. We give explicit finite difference formulas at irregular grid points by virtue of the level set function, and reformulate it in a symmetric form. The difference scheme using IMIB method is shown to satisfy the discrete maximum principle for a certain class of problems. Thus, rigorous proofs of second-order convergence of the IMIB method applied to 1D problems with piecewise constant coefficients and 2D problems with singular sources can be obtained easily. For 1D problems, we obtain a sharp error bound for the approximate solution by comparison function technique, while we do not get the error analysis for 2D problems with piecewise constant coefficients. Numerical examples in Section 4 are also given to support the analytical results.

Acknowledgements

The authors would like to thank Prof. Huaxiong Huang and the anonymous referees for their valuable comments and suggestions which are very important for the revision of this article.

Appendix. The essential equivalence among the IIM, IMIB and second-order interpolation formulation in 1D

For simplicity, we only discuss the difference scheme at irregular point x_k, the case for x_{k+1} is similar.
In the IIM [12], the difference scheme for irregular point x_k can be written as

$$\gamma_{k,1}u_{k-1} + \gamma_{k,2}u_k + \gamma_{k,3}u_{k+1} = f_k + C_k, \tag{A.1}$$

where

$$\gamma_{k,1} = \frac{\beta^- - [\beta](x_k - \alpha)/h}{D_k}, \tag{A.2}$$

$$\gamma_{k,2} = \frac{-2\beta^- + [\beta](x_{k-1} - \alpha)/h}{D_k}, \tag{A.3}$$

$$\gamma_{k,3} = \frac{\beta^+}{D_k}, \tag{A.4}$$

and

$$D_k = h^2 + \frac{[\beta](x_{k-1} - \alpha)(x_k - \alpha)}{2\beta^-}, \tag{A.5}$$

$$C_k = \left(a_\Gamma + (x_{k+1} - \alpha)\frac{b_\Gamma}{\beta^+} + \frac{(x_{k+1} - \alpha)^2}{2\beta^+}[f]\right)\gamma_{k,3}. \tag{A.6}$$

Noting that $\alpha - x_k = \theta h$, $x_{k+1} - \alpha = (1-\theta)h$ and multiplying (A.1) by $\hat{\beta}D_k/(\beta^+h^2)$, we obtain

$$\tilde{\gamma}_{k,1}u_{k-1} + \tilde{\gamma}_{k,2}u_k + \tilde{\gamma}_{k,3}u_{k+1} = \tilde{f}_k + \tilde{C}_k, \tag{A.7}$$

where

$$\tilde{\gamma}_{k,1} = \frac{\hat{\beta}D_k}{\beta^+h^2}\frac{\beta^- - [\beta](x_k - \alpha)/h}{D_k} = \frac{\hat{\beta}(\beta^- + (\beta^+ - \beta^-)\theta)}{\beta^+h^2} = \frac{\beta^-}{h^2}, \tag{A.8}$$

$$\tilde{\gamma}_{k,3} = \frac{\hat{\beta}D_k}{\beta^+h^2}\frac{\beta^+}{D_k} = \frac{\hat{\beta}}{h^2}, \tag{A.9}$$

$$\tilde{\gamma}_{k,2} = \frac{\hat{\beta}D_k}{\beta^+h^2}\frac{-2\beta^- + [\beta](x_{k-1} - \alpha)/h}{D_k} = -\frac{\hat{\beta}D_k}{\beta^+h^2}(\gamma_{k,1} + \gamma_{k,3}) = -\frac{\beta^-}{h^2} - \frac{\hat{\beta}}{h^2}, \tag{A.10}$$

and

$$\tilde{f}_k = \frac{\hat{\beta} D_k}{\beta^+ h^2} f_k = \frac{\hat{\beta}}{\beta^+ h^2}\left(h^2 + \frac{(\beta^+ - \beta^-)\theta(1+\theta)h^2}{2\beta^-}\right) f_k = \frac{\hat{\beta}}{2}\left(\frac{\theta+\theta^2}{\beta^-} + \frac{2-\theta-\theta^2}{\beta^+}\right) f_k, \tag{A.11}$$

$$\tilde{C}_k = \frac{\hat{\beta} D_k}{\beta^+ h^2}\left(a_\Gamma + (x_{k+1}-\alpha)\frac{b_\Gamma}{\beta^+} + \frac{(x_{k+1}-\alpha)^2}{2\beta^+}[f]\right)\gamma_{k,3} \tag{A.12}$$

$$= \frac{\hat{\beta}}{h^2}\left(a_\Gamma + (x_{k+1}-\alpha)\frac{b_\Gamma}{\beta^+} + \frac{(x_{k+1}-\alpha)^2}{2\beta^+}[f]\right) \tag{A.13}$$

$$= \frac{\hat{\beta} a_\Gamma}{h^2} + \frac{\hat{\beta}(1-\theta) b_\Gamma}{\beta^+ h} + \frac{\hat{\beta}(1-\theta)^2}{2\beta^+}[f]. \tag{A.14}$$

Then, it is easy to see that Eq. (A.7) is just the same as (2.35).

In the interpolation formulation of the MIB [27], we know that the difference scheme for irregular point x_k can be written as

$$\beta^- \frac{2a_2^-}{h^2} = f_k. \tag{A.15}$$

The coefficient a_2^- is solved by inverting the coefficient matrix of equation

$$\begin{pmatrix} -1 & 1 & 0 & 0 \\ 0 & 0 & 1 & 1 \\ -x_l & -x_l^2 & -x_r & -x_r^2 \\ -\beta^- & -2\beta^- x_l & \beta^+ & -2\beta^+ x_r \end{pmatrix} \cdot \begin{pmatrix} a_1^- \\ a_2^- \\ a_1^+ \\ a_2^+ \end{pmatrix} = \begin{pmatrix} u_{k-1} - u_k \\ u_{k+2} - u_{k+1} \\ a_\Gamma - u_{k+1} + u_k \\ h * b_\Gamma \end{pmatrix} \tag{A.16}$$

where

$$x_l = \frac{\alpha - x_k}{h} = \theta, \qquad x_r = \frac{x_{k+1} - \alpha}{h} = 1 - \theta. \tag{A.17}$$

It can be solved from (A.16) that

$$\begin{aligned} a_2^- = {} & \frac{1}{2+\theta+3\theta r - 5\theta^2 + \theta^2 r + 2\theta^3 - 2\theta^3 r}\big\{(2+3\theta r - 3\theta - 2\theta^2 r + \theta^2)u_{k-1} \\ & - (3r + 2 + \theta r - 3\theta - 2\theta^2 r + \theta^2)u_k + r(2-\theta)^2 u_{k+1} - r(1-\theta)^2 u_{k+2} - r(3-2\theta)a_\Gamma \\ & - (2 - 3\theta + \theta^2) b_\Gamma h/\beta^-\big\}. \end{aligned} \tag{A.18}$$

Substituting Eq. (A.18) into Eq. (A.15), we obtain the same difference formulation as (2.32).

References

[1] I. Babuska, The finite element method for elliptic equations with discontinuous coeffcients, Computing 5 (1970) 207–213.
[2] Z. Chen, J. Zou, Finite element methods and their convergence for elliptic and parabolic interface problems, Numer. Math. 79 (1998) 175–202.
[3] B. Griffith, C. Peskin, On the order of accuracy of the immersed boundary method: Higher order convergence rates for sufficiently smooth problems, J. Comput. Phys. 208 (2005) 75–105.
[4] M. Lai, C. Peskin, An immersed boundary method with formal second-order accuracy and reduced numerical viscosity, J. Comput. Phys. 160 (2000) 705–719.
[5] C. Peskin, Numerical analysis of blood flow in heart, J. Comput. Phys. 25 (1977) 220–252.
[6] C. Peskin, Lectures on mathematical aspects of physiology, Lect. Appl. Math. 19 (1981) 69–109.
[7] C. Peskin, D. McQueen, A 3-dimensional computational method for blood-flow in the heart. 1. immersed elastic fibers in a viscous incompressible fluid, J. Comput. Phys. 81 (1989) 372–405.
[8] C. Peskin, B. Printz, Improved volume conservation in the computation of flows with immersed elastic boundaries, J. Comput. Phys. 105 (1993) 33–46.
[9] L. Adams, Z. Li, The immersed interface/multigrid methods for interface problems, SIAM J. Sci. Comput. 24 (2002) 463–479.
[10] S. Deng, K. Ito, Z. Li, Three-dimensional elliptic solvers for interface problems and applications, J. Comput. Phys. 184 (2003) 215–243.
[11] J. Sethian, A. Wiegmann, Structural boundary design via level set and immersed interface methods, J. Comput. Phys. 163 (2000) 489–528.
[12] R. Leveque, Z. Li, The immersed interface method for elliptic equations with discontinuous coefficients and singular sources, SIAM J. Numer. Anal. 31 (1994) 1019–1044.
[13] Z. Li, K. Ito, Maximum principle preserving schemes for interface problems with discontinuous coefficients, SIAM J. Sci. Comput. 23 (2001) 339–361.
[14] Z. Li, An overview of the immersed interface method and its application, Taiwan. J. Math. 7 (2003) 1–49.
[15] Z. Li, A fast iterative algorithm for elliptic interface problems, SIAM J. Numer. Anal. 35 (1998) 230–254.
[16] A. Wiegmann, K. Bube, The explicit-jump immersed interface method: Finite difference methods for pdes with piecewise smooth solutions, SIAM J. Numer. Anal. 37 (2000) 827–862.
[17] Z. Li, The immersed interface method using a finite element formulation, Appl. Numer. Math. 27 (1998) 253–267.
[18] S. Hou, X. Liu, A numerical method for solving variable cofficient elliptic equation with interfaces, J. Comput. Phys. 202 (2005) 411–445.
[19] H. Huang, Z. Li, Convergence analysis of the immersed interface method, IMA J. Numer. Anal. 19 (1999) 583–608.

[20] R. Fedkiw, T. Aslam, B. Merriman, S. Osher, A non-oscillatory eulerian approach to interfaces in multimaterial flows (the ghost fluid method), J. Comput. Phys. 152 (1999) 457–492.
[21] X. Liu, R. Fedkiw, M. Kang, A boundary condition capturing method for poissons equation on irregular domains, J. Comput. Phys. 160 (2000) 151–178.
[22] M. Kang, R. Fedkiw, X. Liu, A boundary condition capuring method for multiphase incompressible flow, J. Sci. Comput. 15 (2000) 323–360.
[23] S. Yu, Y. Zhou, G. Wei, Matched interface and boundary (MIB) method for elliptic problems with sharp-edged interfaces, J. Comput. Phys. 224 (2007) 729–756.
[24] S. Yu, G. Wei, Three-dimensional mathed interface and boundary (MIB) method for treating geometric singularities, J. Comput. Phys. 227 (2007) 602–623.
[25] S. Zhao, G. Wei, High order FDTD methods via derivative matching for maxwell equations with material interfaces, J. Comput. Phys. 200 (2004) 60–103.
[26] Y. Zhou, S. Zhao, M. Feig, G. Wei, High order matched interface and boundary method for elliptic equations with discontinuous coefficients and singular sources, J. Comput. Phys. 213 (2006) 1–30.
[27] Y. Zhou, G. Wei, On the fictious-domain and interpolation formulations of the matched interface and boundary method, J. Comput. Phys. 219 (2006) 228–246.
[28] J. Bramble, J. King, A finite element method for interface problems in domains with smooth boundaries and interfaces, Adv. Comput. Math. 6 (1996) 109–138.
[29] Z. Li, T. Lin, et al., New cartesian grid methods for interface problems using the finite element formulation, Numer. Math. 96 (2003) 61–98.
[30] W. Liu, Y. Liu, et al., Immersed finite element method and its applications to biological systems, Comput. Methods Appl. Mech. Eng. 195 (2006) 1722–1749.
[31] R. Sinha, B. Deka, On the convergence of finite element method for second order elliptic interface problems, Numer. Funct. Anal. Optim. 27 (2006) 99–115.
[32] J. Huang, J. Zou, A mortar element method for elliptic problems with discontinuous coefficients, IMA J. Numer. Anal. 22 (2002) 549–576.
[33] W. Wang, A jump condition capturing finite difference scheme for elliptic interface problems, SIAM J. Sci. Comput. 25 (2004) 1479–1496.
[34] Z. Li, W. Wang, I. Chern, M. Lai, New formulations for interface problems in polar coordinates, SIAM J. Sci. Comput. 25 (2003) 224–245.
[35] S. Yu, W. Geng, G. Wei, Treatment of geometric singularities in the implicit solvent models, J. Chem. Phys. 126 (2007) 244108.
[36] X. Liu, T.C. Sideris, Convergence of the ghost fluid method for elliptic equations with interfaces, Math. Comput. 72 (2003) 1731–1746.
[37] B. Fornberg, Calculation of weights in finite difference formulas, SIAM Rev. 40 (1998) 685–691.
[38] P. Ciarlet, Discrete maximum principles for finite difference operators, Aequationes Math. 4 (1970) 336–352.